

Supporting Information:

Ultrahigh average ZT realized in p -type SnSe crystalline thermoelectrics through producing extrinsic vacancies

Bingchao Qin,¹ Yang Zhang,² Dongyang Wang,¹ Qian Zhao,¹ Bingchuan Gu,³ Haijun Wu,^{2,*}
Hongjun Zhang,^{3,*} Bangjiao Ye,³ Stephen J. Pennycook,² Li-Dong Zhao^{1,**}

¹*School of Materials Science and Engineering, Beihang University, Beijing 100191, China*

²*Department of Materials Science and Engineering, National University of Singapore, 117575, Singapore*

³*State Key Laboratory of Particle Detection and Electronics & Hefei National Laboratory for Physical Sciences at the Microscale, University of Science and Technology of China, Hefei 230026, China*

Corresponding authors:

wu.haijun@u.nus.edu;

hjzhang8@ustc.edu.cn;

zhaolidong@buaa.edu.cn (Lead Contact)

Experimental Details

Raw materials: Sn granules (99.999%, Aladdin element, China), Se pieces (99.999%, Aladdin element, China), Na blocks (99.95%, Aladdin element, China).

Synthesis: In this work, we choose 1.5% mol Na as effective dopants for all samples since it was determined as the optimized doping fraction.¹ We firstly synthesized polycrystalline SnSe₂ using melting method.² The high-purity powders of Sn and Se were weighed according to the stoichiometric ratio of SnSe₂ and the mixed powders were sealed in evacuated quartz tubes and heated slowly up to 1023 K. The tubes were held at this temperature for 24 h and then quenched rapidly to room temperature in cold water. The obtained polycrystalline SnSe₂ was used for further synthesizing SnSe+xSnSe₂ crystal samples. Next, high-purity elemental constituents of Sn, Se, SnSe₂, and Na were weighted in a stoichiometric ratio of Sn_{0.985}Na_{0.015}Se + x% SnSe₂ (x = 1, 2, 3, and 5, since Na doping fraction is fixed, in this paper, Sn_{0.985}Na_{0.015}Se + x% SnSe₂ was shortly named as SnSe + xSnSe₂ (x = 1, 2, 3, and 5). The starting chemicals were loaded into carbon-coated conical silicon tubes under a glove box with nitrogen atmosphere. The tubes were evacuated and flame-sealed under pressure of $\sim 10^{-4}$ Pa. The outer tubes were used to prevent samples from oxidation because the inner tubes could break caused by high-temperature phase transition. The tubes were then loaded into vertical furnace, heated up to 1313 K at rate of 10 Kmin⁻¹ and soaked for 10 h, subsequently cooled to 1073 K at a slow rate of 1 Kh⁻¹ and furnace cooled to room temperature. Finally, the SnSe + SnSe₂ crystals with diameter of ~ 12 mm and length of ~ 30 mm were obtained.

X-ray diffraction and X-ray back-reflection Laue: Samples pulverized with an agate mortar were used for X-ray powder diffraction. The diffraction patterns were recorded with Cu K _{α} ($\lambda = 1.5418$ Å) radiation in a reflection geometry on an Inel diffractometer operating at 40 kV and 20 mA using a position-sensitive detector. The cleavage plane (100) of SnSe + SnSe₂ crystals were detected by X-ray back-reflection Laue to determine the in-plane (*b-c* plane) orientations. The crystals are placed according to their growth direction and their cleavage planes are facing to X-ray resource. The Laue patterns were obtained through collecting diffraction lines by a plate on a diffractometer operating at 20 kV and 18 mA. The thermoelectric transport parameters were measured along the *b*-axis direction.

Bandgap measurements: Room temperature optical diffuse reflectance spectra of the powder were obtained on a UV–vis-NIR Spectrophotometer (UV-3600 Plus) equipped with a polytetrafluoroethylene (PTFE) integrating sphere (ISR-603 integrating sphere). Samples ground into powders were spread on a plate surface compacted with BaSO₄ powders. In order to estimate the bandgap of samples, the reflectance versus wavelength data given in the diffuse reflectance spectra was converted to absorption data using Kubelka–Munk equations: $\alpha/S = (1-R)^2/2R$, where R , α and S represents the reflectance, the absorption and scattering coefficients, respectively.

Electrical transport properties: The obtained SnSe + SnSe₂ crystals were cut into bars with $3 \times 3 \times 8 \text{ mm}^3$ that were used for simultaneous measurements of the electrical conductivity and Seebeck coefficient using Cryoall CTA and Ulvac Riko ZEM-3 instruments under a helium atmosphere from room temperature to 773 K. The samples were coated with a thin layer of boron nitride (BN) to protect the instruments from the possible evaporation of samples. The uncertainty of the Seebeck coefficient and electrical conductivity measurement is within 5 %.

Thermal transport properties: The obtained SnSe + SnSe₂ crystals were cut and polished into a $\Phi 6 \text{ mm}$ disk shape with a 1–2 mm thickness for thermal diffusivity measurements. The disks were coated with a thin layer of graphite to minimize errors from the emissivity of the materials. The thermal conductivity was calculated according to the formula $\kappa = D \cdot \rho \cdot C_p$, where the thermal diffusivity (D) was measured using laser flash diffusivity method with a Netzsch LFA457 instrument, ρ is the sample density determined using the dimensions and mass of the sample and then reconfirmed using a gas pycnometer (Micromeritics AccuPyc II 1340) measurements (shown in **Table S2**), and C_p is the specific heat capacity obtained from Debye model.³ The thermal diffusivity data were analyzed using a Cowan model with pulse correction. The uncertainty of the thermal conductivity is estimated to be within 8 %, considering all the uncertainties from D , ρ and C_p . The combined uncertainty for all measurements involved in the calculation of ZT is within 20 %.

Hall measurement: Hall coefficients (R_H) were measured under a reversible magnetic field (1 T) by the Van der Pauw method by using a Hall measurement system (Lake Shore 8400 Series, Model 8404, USA) at 300-793K. Carrier density (n_H) was obtained by $n_H = 1/(e \cdot R_H)$, and carrier mobility (μ_H) was calculated using the relationship $\mu_H = \sigma \cdot R_H$ with σ being the

electrical conductivity obtained from Cryoall CTA and Ulvac Riko ZEM-3 instruments.

Positron Annihilation Lifetime (PAL) measurements: The PAL measurements were carried out by using an ORTEC fast-fast coincidence system with a time resolution of around 230 ps in full width at half maximum (FWHM). The total counts of 2×10^6 were collected for each PAL spectrum. A ^{22}Na positron source (about 30 μCi) was sandwiched between two identical SnSe pellet-shaped samples.

Density functional theory (DFT) calculations: DFT calculations were conducted to obtain the theoretical lifetimes. The atomic superposition (ATSUP) method was used to calculate the electron density and positron crystalline Coulomb potential which were constructed by the non-self-consistent superposition of free atom electron density and Coulomb potential in the absence of the positron.⁴⁻⁵ And then the Quantum Monte Carlo Generalized Gradient Approximation (QMCGGA) form of the enhancement factor was chosen to calculate the positron annihilation parameters.⁶ The model of $2 \times 2 \times 2$ supercells was used for the calculations of SnSe based compound with unrelaxed structure vacancy.

Microstructure characterization: The specimens were prepared by conventional standard methods, that is, cutting, grinding, dimpling, polishing and Ar-ion milling with a liquid nitrogen cooling stage. (Scanning) transmission electron microscopy (STEM and TEM) and energy dispersive X-ray spectroscopy (EDS) studies were conducted using a JEOL ARM200F atomic resolution analytical electron microscope installed in the National University of Singapore equipped with a cold field-emission gun, a new ASCOR 5th order aberration corrector and Gatan OneView camera and an Oxford X-Max 100TLE X-ray detector.

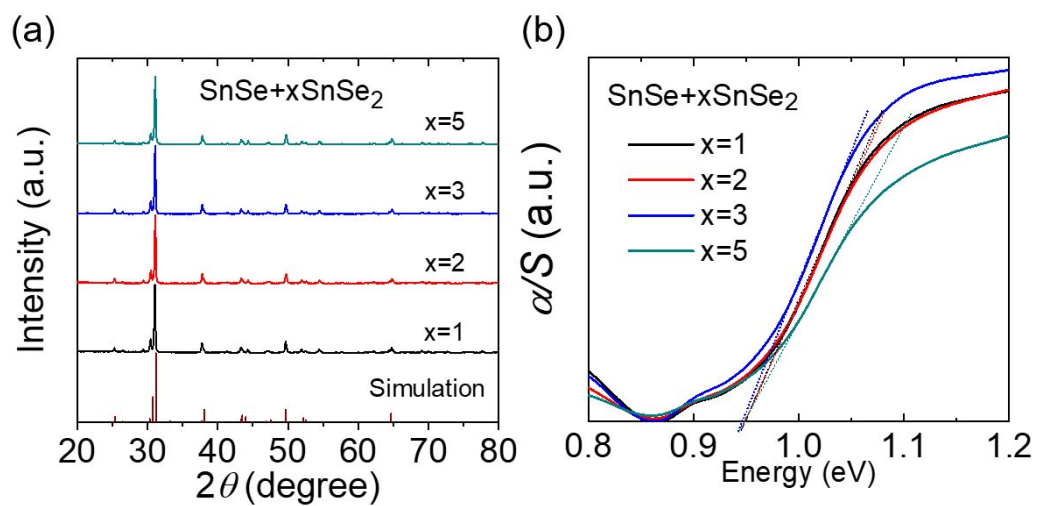


Figure S1. (a) Powder XRD patterns and (b) Optical absorption spectra for $\text{SnSe}+x\text{SnSe}_2$ samples.

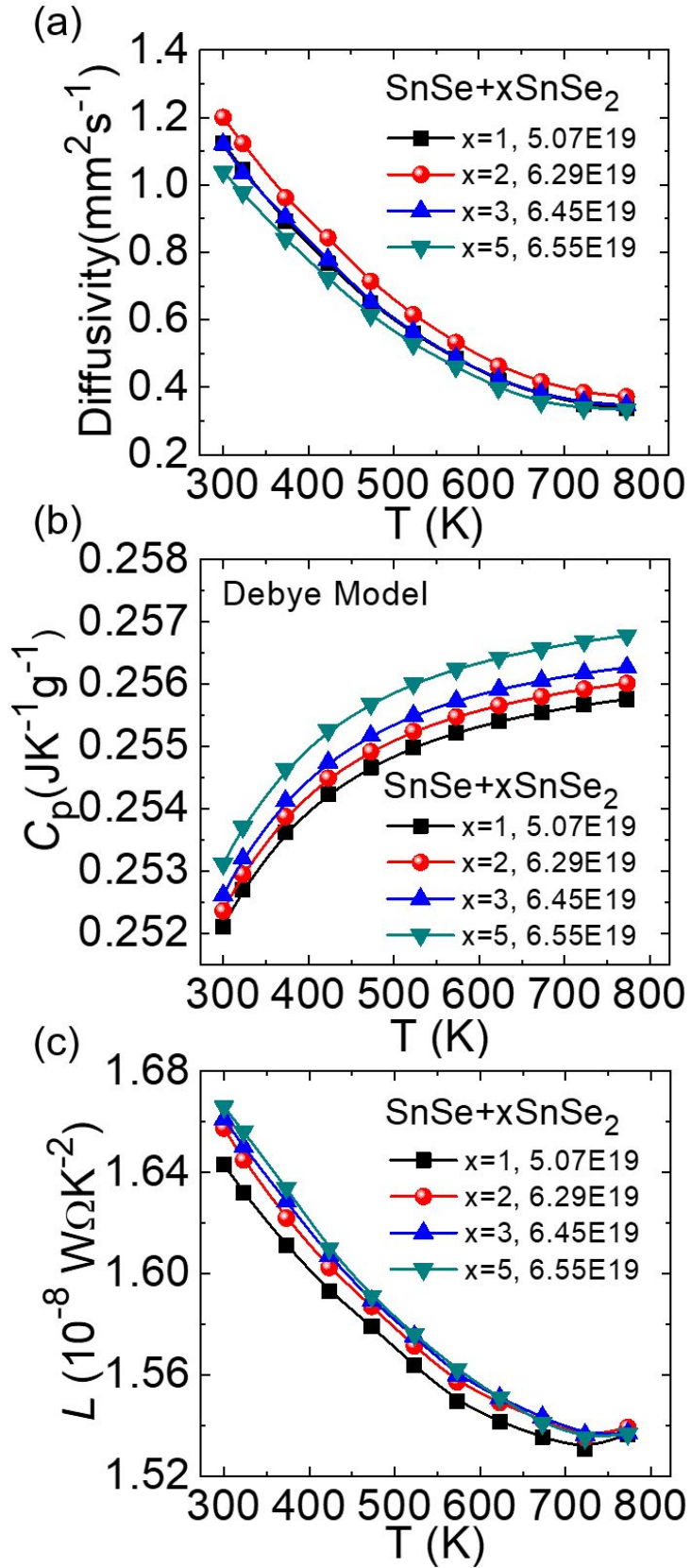


Figure S2. Thermoelectric transport properties as a function of temperature for SnSe+xSnSe₂ samples: (a) Thermal diffusivity; (b) Specific heat calculated using Debye Model; (c) Lorenz number.

Table S1. Room temperature Hall data of SnSe + xSnSe₂ samples.

Samples	σ (S cm ⁻¹)	n_H ($\times 10^{19}$ cm ⁻³)	μ_H (cm ² V ⁻¹ s ⁻¹)
x=1	1273.58	5.07	157.00
x=2	1606.83	6.29	159.66
x=3	1464.78	6.45	141.94
x=5	1316.10	6.55	125.58

Table S2. Experimental densities of SnSe + xSnSe₂ samples.

Samples	ρ (gcm ⁻³)
x=1	5.86
x=2	5.89
x=3	5.91
x=5	5.88

Calculations on the carrier concentration dependent ZT values

The single band model was adopted to calculate the relationship between ZT s and carrier concentrations (n_H) at given temperatures.⁷⁻⁸ The relationship between Seebeck coefficient (S) and carrier concentration (n_H) is presented as follows:

$$S = \frac{k_B}{e} \left(\frac{(2 + \lambda)F_{1+\lambda}(\eta)}{(1 + \lambda)F_{\lambda}(\eta)} - \eta \right) \quad (S1)$$

$$n_H = 4\pi \left(\frac{2m^* kT}{h^2} \right)^{\frac{3}{2}} F_{\frac{1}{2}}(\eta) \quad (S2)$$

$$F_j(\eta) = \int_0^{\infty} \frac{\zeta^j d\zeta}{1 + \exp[\zeta - \eta]} \quad (S3)$$

where k_B is the Boltzmann constant, e is the electron charge, η is the chemical potential, h is the Planck constant and λ is the phonon scattering factor. The scattering factor (λ) is -1/2 as acoustic phonon scattering is generally assumed the dominant scattering mechanism. $F_j(\eta)$ is the j -th Fermi integral, and ζ is the reduced carrier energy. The reduced Fermi energy η is determined based on the fitting of the Seebeck coefficients.

The band effective masses of SnSe + 2SnSe₂ sample in this work at different temperatures (300 K, 600 K and 773 K) are obtained by fitting experimental data into Equations S1, S2 and S3. The electrical conductivity is determined by $\sigma = e n_H \mu_H$, in which the Hall carrier mobility (μ_H) is calculated by the following Equation S4,

$$\mu_H = \mu_0 \frac{\left(\frac{1}{2} + 2\lambda \right) F_{2\lambda - \frac{1}{2}}(\eta)}{(1 + \lambda) F_{\lambda}(\eta)} \quad (S4)$$

where μ_0 is the measured carrier mobility at given temperatures.

Total thermal conductivity (κ_{tot}) includes lattice (κ_{lat}) and electronic (κ_{ele}) thermal conductivity. The lattice thermal conductivity is independent with carrier concentration and keeps as constant at each given temperature. κ_{ele} is in proportion to the electrical conductivity and temperature according to the Wiedeman-Franz relation, $\kappa_{\text{ele}} = L\sigma T$, where the Lorenz number L can be evaluated as follow,

$$L = \frac{k^2 3F_0(\eta)F_2(\eta) - 4F_1(\eta)^2}{e^2 F_0(\eta)^2} \quad (S5)$$

Thus, the carrier concentration dependent S , σ and κ_{ele} can be obtained and the carrier concentration dependent ZT s can be evaluated, as shown in **Figure 8(b)**.

REFERENCES

1. Zhao, L.-D.; Tan, G.; Hao, S.; He, J.; Pei, Y.; Chi, H.; Wang, H.; Gong, S.; Xu, H.; Dravid, V. P.; Uher, C.; Snyder, G. J.; Wolverton, C.; Kanatzidis, M. G., Ultrahigh power factor and thermoelectric performance in hole-doped single-crystal SnSe. *Science* **2016**, *351* (6269), 141-144.
2. Shu, Y.; Su, X.; Xie, H.; Zheng, G.; Liu, W.; Yan, Y.; Luo, T.; Yang, X.; Yang, D.; Uher, C.; Tang, X., Modification of Bulk Heterojunction and Cl Doping for High-Performance Thermoelectric SnSe₂/SnSe Nanocomposites. *ACS Applied Materials & Interfaces* **2018**, *10* (18), 15793-15802.
3. Qin, B.; Wang, D.; He, W.; Zhang, Y.; Wu, H.; Pennycook, S. J.; Zhao, L.-D., Realizing High Thermoelectric Performance in p-Type SnSe through Crystal Structure Modification. *Journal of the American Chemical Society* **2019**, *141* (2), 1141-1149.
4. Puska, M. J.; Nieminen, R. M., Defect spectroscopy with positrons: a general calculational method. *Journal of Physics F: Metal Physics* **1983**, *13* (2), 333-346.
5. Seitsonen, A. P.; Puska, M. J.; Nieminen, R. M., Real-space electronic-structure calculations: Combination of the finite-difference and conjugate-gradient methods. *Physical Review B* **1995**, *51* (20), 14057-14061.
6. Zhang, W.; Gu, B.; Liu, J.; Ye, B., Accurate theoretical prediction on positron lifetime of bulk materials. *Computational Materials Science* **2015**, *105*, 32-38.
7. Toberer, E. S.; Zevalkink, A.; Crisosto, N.; Snyder, G. J., The Zintl Compound Ca₅Al₂Sb₆ for Low-Cost Thermoelectric Power Generation. *Advanced Functional Materials* **2010**, *20* (24), 4375-4380.
8. Zhao, Q.; Wang, D.; Qin, B.; Wang, G.; Qiu, Y.; Zhao, L.-D., Synergistically optimized electrical and thermal transport properties of polycrystalline SnSe via alloying SnS. *Journal of Solid State Chemistry* **2019**, *273*, 85-91.